Interfacial Phenomena and Heat Transfer, 5(4):299–308 (2017)

SIMULATION OF PHASE CHANGE PROCESS IN CAPILLARY TUBES WITH A HYBRID LATTICE BOLTZMANN METHOD

Guancui Zhong, Hongtao Gao, & Bingbing Liu*

Institute of Refrigeration and Cryogenics Engineering, Dalian Maritime University, 116026, Dalian, China

*Address all correspondence to: Hongtao Gao, Institute of Refrigeration and Cryogenics Engineering, Dalian Maritime University, Dalian, 116026, China; Tel.: +86 411 8472 3126,
E-mail: gaohongtao@dlmu.edu.cn

Original Manuscript Submitted: 10/31/2017; Final Draft Received: 5/1/2018

In this article the mesoscopic lattice Boltzmann method (LBM) is used to simulate the flow in a rectangular capillary tube. Combining the free energy model with the thermal model, a hybrid LBM is proposed for two-phase fluids. This hybrid LBM is used to simulate the gas-liquid phase change process of capillary tube flows. The consequences show that the temperature of the center of the tube is higher than that of the circumferential wall before the phase change. The phase change starts at the center of the tube, then the gas expands along the axial direction of the capillary tube, and finally the center of the entire tube is almost filled with the gas. In gas-liquid two-phase flow of the capillary tube, the velocity of gas is much higher than that of liquid. It is found that the pressure drop has a great influence on gas-liquid phase change of the capillary tube.

KEY WORDS: *lattice Boltzmann method, gas-liquid phase change, capillary tubes*

1. INTRODUCTION

Capillary tubes are a typical throttling element, which were proposed by Staebler (1948) in the 1930s and patented in 1942. The capillary tube connects the condenser to the evaporator, and liquid refrigerant flows from the side condenser to the side evaporator and expands down to the evaporator pressure. In addition, it has the function of controlling the superheated and evaporating liquid level, which has a great influence on the performance of a refrigeration system. Usually, capillary tubes have diameters ranging from 0.5 to 2.0 mm and lengths from 2 to 6 m (Khan et al., 2009). Owing to its simplicity and low cost, capillary tubes have become the most common throttling element of household refrigerating systems.

Over the past seven decades, people have made a lot of theoretical and experimental studies on capillary throttling. Bolstad and Jordan (1948) were early scholars studying the flow characteristic of capillary tubes. They obtained the pressure and temperature distribution curve along the capillary. The database for R600a mass flow of adiabatic capillary tubes has been expanded by Schenk and Oellrich (2014). Fiorelli et al. (2002) have researched the performance of R-407C and R-410A flowing through the adiabatic capillary tubes, which was carried out for both subcooled and two-phase inlet conditions. Wongwises et al. (2000) have proposed a numerical simulation model based on the homogeneous two-phase flow model and compared the flow characteristics of refrigerants R-12, R22, and R-502. Deodhar et al. (2015) have studied local pressure variation in an adiabatic straight capillary tube experimentally, with R134a as the working fluid. It was found that the diameter is the most sensitive design parameter of the capillary tube. Most of these studies analyzed the flow characteristics of capillary tube focusing on pressure and temperature of the inlet and the outlet, diameter, length, and mass flow.

With the improvement of visualization technology, many researchers begin to analyze the gas-liquid two-phase flow of the capillary microchannel by using a high-speed camera. Cooper et al. (1957) firstly found that gas-liquid

NOMENCLATURE

c_i	velocity vectors of LBM	Δx	spacing of the cubic lattice
Ja	Jacob number		
P	pressure of the fluid		
Pe	Péclet number	**Greek Symbols**	
T	temperature of the fluid	$\delta_{\alpha\beta}$	Kronecker delta
Δt	discrete time	μ	viscosity of fluid
u	macroscopic velocity of the fluid	ρ	density of fluid
u^*	predicted velocity	ϕ	order parameter

two-phase flow in a capillary was a fog flow according to visualization experiments. Koizumi and Yokoyama (1980) also made a visual study of the capillary, and considered that the two-phase flow of the capillary was a high-speed foam flow. At present, many researchers have done a lot of studies on the visualization experiment of capillary two-phase flow. Many experiments have studied the flow pattern transition by mixing gas (usually air or nitrogen) and liquid into a microchannel (Triplett et al., 1999; Ewing et al., 1999; Liu et al., 2016), or by heating the refrigerant to produce gas in the tube to study the flow characteristic of the capillary tube (Revellin et al., 2006; Oliveira et al., 2016). However, these experimental processes cannot be regarded as the capillary throttling process of the refrigeration system. Due to the existence of these limitations and the complexity of the gas-liquid two-phase flow in the capillary, there is a lack of comprehensive understanding of the two-phase flow mechanism in the tube. Thererfore, there is still a lot of work to do in the study of gas-liquid phase change in capillary tubes.

Many researchers have studied flow characteristics of capillary tubes from a macroscopic view, but the distributions of physical parameters such as velocity, pressure, temperature, and density in the capillary in the phase change process were rarely considered. In this study, from a microcosmic view the details of phase change of the capillary are studied with the lattice Boltzmann method. Compared with the volume of fluid (VOF) method, the lattice Boltzmann method based on discrete kinetic theory is more accurate to catch a multiphase interface, and compared with molecular dynamics simulation, it does not focus on every fluid molecule, which can reduce the computation cost. Owing to its simplicity and high computational efficiency, the lattice Boltzmann method has been widely used in direct simulation of multiphase flows (Huang et al., 2017).

In this research, by using the lattice Boltzmann method as a numerical simulation method, the distributions of physical parameters such as density, temperature, pressure, and velocity in the process of capillary throttle flow are obtained. The numerical model of this study has some reference value to research the mechanism of microchannel throttling with the lattice Boltzmann method.

2. NUMERICAL METHOD

A new model of gas-liquid phase change model is proposed to simulate the phase change process of capillary flow in this study, which is based on the a free energy model for two-phase fluids with large density differences (Inamuro et al., 2004) and on a thermal model, both of which were proposed by Inamuro (2006).

2.1 Free Energy Model

Regular discrete lattices are usually used in the lattice Boltzmann model, which specifies that the particles move along the lattice line and collide at the lattice point. The D3Q15 model is used (N = 15) in the present paper. The velocity

vectors of this model are given by Eq. (1).

$$c_i = \begin{bmatrix} 0 & 1 & 0 & 0 & -1 & 0 & 0 & 1 & -1 & 1 & 1 & -1 & 1 & -1 & -1 \\ 0 & 0 & 1 & 0 & 0 & -1 & 0 & 1 & 1 & -1 & 1 & -1 & -1 & 1 & -1 \\ 0 & 0 & 0 & 1 & 0 & 0 & -1 & 1 & 1 & 1 & -1 & -1 & -1 & -1 & 1 \end{bmatrix}. \tag{1}$$

In the free energy model, two particle velocity distribution functions f_i and g_i are used. The function f_i is used for the calculation of an order parameter which distinguishes two phases, and the function g_i is used for the calculation of velocity of the two-phase fluids. The evolution of particle distribution functions f_i and g_i are given by Eqs. (2) and (3).

$$f_i(x + c_i\delta_t, t + \delta_t) = f_i(x,t) - \frac{1}{\tau_f}\left[f_i(x,t) - f_i^{eq}(x,t)\right], \tag{2}$$

$$g_i(x + c_i\delta_t, t + \delta_t) = g_i(x,t) - \frac{1}{\tau_g}\left[g_i(x,t) - g_i^{eq}(x,t)\right] + 3E_i c_{ia}\frac{1}{\rho}\left[\frac{\partial}{\partial x_\beta}\left\{\mu\left(\frac{\partial \mu_\beta}{\partial x_\alpha} + \frac{\partial \mu_\alpha}{\partial x_\beta}\right)\right\}\right]\Delta x. \tag{3}$$

The change of velocity is due to external force, so the external force term is added to Eq. (3) as the last term on the right side, where f_i^{eq} and g_i^{eq} are the discrete equilibrium distribution functions, which can be obtained by Eqs. (4) and (5).

$$f_i^{eq} = H_i\phi + F_i\left[P_0 - k_f\phi\frac{\partial^2\phi}{\partial x_\alpha^2} - \frac{k_f}{6}\left(\frac{\partial\phi}{\partial x_\alpha}\right)^2\right] + 3E_i\phi c_{i\alpha}u_\alpha + E_i k_f G_{\alpha\beta}(\phi)c_{i\alpha}c_{i\beta}, \tag{4}$$

$$\begin{aligned} g_i^{eq} = {} & E_i\left[1 + 3c_{i\alpha}u_\alpha - \frac{3}{2}u_\alpha u_\alpha + \frac{9}{2}c_{i\alpha}c_{i\beta}u_\alpha u_\beta + \frac{3}{2}\left(\tau_g - \frac{1}{2}\right)\delta_x\left(\frac{\partial u_\beta}{\partial u_\alpha} + \frac{\partial u_\alpha}{\partial u_\beta}\right)c_{i\alpha}c_{i\beta}\right] \\ & + E_i\frac{k_g}{\rho}G_{\alpha\beta}(\rho)c_{i\alpha}c_{i\beta} - \frac{3}{2}F_i\frac{k_g}{\rho}\left(\frac{\partial\rho}{\partial x_\alpha}\right)^2, \end{aligned} \tag{5}$$

where

$$P_0 = \phi\frac{T}{1 - b\phi} - a\phi^2, \tag{6}$$

$$G_{\alpha\beta}(\varphi) = \frac{9}{2}\frac{\partial\varphi}{\partial x_\alpha}\frac{\partial\varphi}{\partial x_\beta} - \frac{3}{2}\frac{\partial\varphi}{\partial x_\gamma}\frac{\partial\varphi}{\partial x_\gamma}\delta_{\alpha\beta}, \tag{7}$$

$$a = 1, \quad b = 6.7, \quad T = 3.5 \times 10^{-2}, \tag{8}$$

$$E_1 = \frac{2}{9}, \quad E_2 \sim E_7 = \frac{1}{9}, \quad E_8 \sim E_{15} = \frac{1}{72}, \tag{9}$$

$$H_1 = 1, \quad H_2 \sim H_{15} = 0, \tag{10}$$

$$F_1 = -\frac{7}{3}, \quad F_i = 3E_i, \quad (i = 2 \sim 15), \tag{11}$$

where τ_f and τ_g are dimensionless single relaxation times, k_f is a constant parameter controlling the width of the interface, and k_g is a constant parameter relating to the strength of the surface tension. The order parameter ϕ distinguishing two phases and the predicted velocity u^* can be obtained in terms of two particle velocity distribution functions as follows:

$$\phi = \sum_{i=1}^{15} f_i, \tag{12}$$

$$u^* = \sum_{i=1}^{15} c_i g_i. \tag{13}$$

The cutoff values of the order parameter, ϕ_G^* and ϕ_L^*, are used to obtain the density in the interface, and the relation between density and gas-liquid two phase is determined by

$$\rho = \begin{cases} \rho_G & \phi < \phi_G^* \\ \dfrac{\Delta\rho}{2}\left[\sin\left(\dfrac{\phi - \overline{\phi^*}}{\Delta\phi^*}\pi\right) + 1\right] + \rho_G, & \phi_G^* \leqslant \phi \leqslant \phi_L^* \\ \rho_L & \phi > \phi_L^* \end{cases}, \tag{14}$$

where ϕ_G^* and ϕ_L^* are the cutoff values of the order parameter, $\phi_G^* = 1.5 \times 10^{-2}$, $\phi_L^* = 9.2 \times 10^{-2}$; ρ_G and ρ_L are the density of gas and liquid, respectively, where $\Delta\rho = \rho_G - \rho_L$, $\Delta\phi = \phi_L^* - \phi_G^*$, and $\overline{\phi^*} = (\phi_L^* - \phi_G^*)/2$. The dynamic viscosity μ at the interface is given by

$$\mu = \frac{\rho - \rho_G}{\rho_L - \rho_G}(\mu_L - \mu_G) + \mu_G. \tag{15}$$

The velocity obtained by Eq. (13) does not take into account the pressure gradient; in order to obtain accurate velocity, pressure gradient must be considered. The following evolution equation of the distribution function h_i is used for the calculation of the pressure P:

$$h_i^{n+1}(x + c_i\delta_t) = h_i^n(x) - \frac{1}{\tau_h}\left[h_i^n(x) - h_i^{eq}(x)\right] - \frac{1}{3}E_i\nabla\cdot\mathrm{u}^*. \tag{16}$$

The corresponding equilibrium distribution function h_i^{eq} is expressed as follows:

$$h_i^{eq} = E_i P^n(x), \tag{17}$$

where n is the number of iterations, and the relaxation time τ_h is given by

$$\tau_h = \frac{1}{\rho} + \frac{1}{2}. \tag{18}$$

The pressure is obtained by

$$p^n = \sum_{i=1}^{15} h_i^n. \tag{19}$$

The pressure convergence criterion is given as follows:

$$\left|\rho^{n+1} - \rho^n\right|/\rho < \varepsilon. \tag{20}$$

Finally the accurate velocity is obtained by

$$\mathrm{u} = \mathrm{u}^* - \frac{\delta_t}{\rho\cdot sh}\nabla P. \tag{21}$$

2.2 Thermal LBM Model

The above LBM is an athermal model; in order to obtain the temperature field, the thermal model proposed by Inamuro (2006) is used in this paper. The evolution equation of temperature is shown as Eq. (22):

$$t_i(x + c_i\delta_t, t + \delta_t) = t_i(x,t) - \frac{1}{\tau_t}[t_i(x,t) - t_i^{eq}(x,t)], \tag{22}$$

where t_i^c is the discrete equilibrium distribution functions given by

$$t_i^{eq} = E_i T(1 + 3c_i\cdot u), \tag{23}$$

where T is the temperature of the fluid, and u is the velocity of the fluid.

The temperature is obtained by

$$T = \sum_{i=1}^{15} t_i. \tag{24}$$

2.3 Hybrid LBM Model

In the free energy model, the gas-liquid interface can be traced by the order parameter. In the continuous transformation theory of Landau, the phase change process can be considered as a continuous change of the order parameter. Therefore, the phase change can be treated by calculating the change of the order parameter. At the same time, the corresponding phase change latent term is added to the thermal LBM model to define the latent heat of the phase change. Combining the free energy model with the thermal LBM model, a hybrid LBM is proposed for the gas-liquid phase change.

In this hybrid LBM model, the phase change term is introduced into Eq. (2). The latent heat is also added to Eq. (22), which is shown below. By hybrid LBM model, the physical quantities such as temperature, density, velocity, and pressure can be coupled.

$$f_i\left(x+c_i\delta_t,t+\Delta t\right)=f_i(x,t)-\frac{1}{\tau_f}\left[f_i\left(x,t\right)-f_i^{eq}\left(x,t\right)\right]+E_i\dot{\phi}, \tag{25}$$

$$t_i\left(x+c_i\delta_t,t+\Delta t\right)=t_i(x,t)-\frac{1}{\tau_t}\left[t_i\left(x,t\right)-t_i^{eq}\left(x,t\right)\right]+E_i\frac{1}{\mathrm{Pe}}\left(\frac{\partial^2 T}{\partial^2 x}\right). \tag{26}$$

In Eq. (25), $\dot{\phi}$ is given by

$$\dot{\phi}=-\frac{\left(\rho_L-\rho_G\right)\rho_L}{\rho_G}\frac{\mathrm{Ja}}{\mathrm{Pe}}\left(\frac{\partial^2 T}{\partial x^2}\right), \tag{27}$$

where Ja is the ratio of latent heat to latent heat of vaporization in the process of the gas-liquid phase change, which is an important parameter for flash evaporation. In the thermal LBM model, the Péclet number Pe is given by

$$\mathrm{Pe}=\frac{3}{\left(\tau_t-0.5\right)\delta_x}. \tag{28}$$

All the first and second derivatives involved in the equations in this study are solved by the following finite-difference approximations:

$$\frac{\partial\varphi}{\partial x_\alpha}\approx\frac{1}{10\delta_x}\sum_{i=2}^{15}c_{i\alpha}\varphi(x+c_i\delta_t), \tag{29}$$

$$\frac{\partial^2\varphi}{\partial x_\alpha}\approx\frac{1}{5\delta_x}\left[\sum_{i=2}^{15}\varphi\left(x+c_i\delta_t\right)-14\varphi\left(x\right)\right]. \tag{30}$$

2.4 Algorithm of Computation

The algorithm of computation can be summarized in six steps.

1. According to calculation conditions, initialize the flow field, and compute the equilibrium distribution functions $f_i^{eq}\left(x,t\right)$, $g_i^{eq}\left(x,t\right)$, $t_i^{eq}\left(x,t\right)$ with Eqs. (4), (5), and (23).
2. Using Eqs. (2), (3), and (22), compute $f_i\left(x,t+\delta_t\right)$, $g_i\left(x,t+\delta_t\right)$, and $t_i\left(x,t+\delta_t\right)$; then compute $\phi\left(x,t+\delta_t\right)$, $u^*\left(x,t+\delta_t\right)$, and $T\left(x,t+\delta_t\right)$ with Eqs. (12), (13), and (24); $\rho\left(x,t+\delta_t\right)$ is calculated with Eq. (14).
3. Using Eq. (16) with Eqs. (17)–(19), compute $P\left(x,t+\delta_t\right)$; the iteration is repeated until Eq. (20) is satisfied in the whole domain.
4. Using Eq. (21), compute $\mathrm{u}\left(x,t+\delta_t\right)$.
5. Calculate the equilibrium distribution functions $f_i^{eq}\left(x,t+\delta_t\right)$, $g_i^{eq}\left(x,t+\delta_t\right)$, and $t_i^{eq}\left(x,t+\delta_t\right)$ with Eqs. (4), (5), and (23).
6. Advance one time step and return to Step 2.

3. NUMERICAL RESULTS AND ANALYSIS

3.1 Density Distribution

In the present paper, a set of experimental data about R600a was used as simulation conditions (Schenk et al., 2014). The gas-liquid density ratio of R600a is 1:50. This study only focuses on the process of the phase change of the capillary throttle, and ignores the other secondary factors. Therefore, the initial state of the calculation domain is the saturated liquid state, the inlet and the outlet velocities are 0 m/s, the fluid temperature is 32°C, the inlet pressure is set to the saturation pressure Pa $= 4.277 \times 10^5$ Pa, and the outlet pressure is Ps $= 7.3 \times 10^4$ Pa.

The simulation domain is a $51 \times 11 \times 11$ cube. The outermost layer of the cube is the boundary, and the interior is liquid. On the surrounding walls, the distribution functions f_i, g_i, t_i, h_i are set as the rebound wall boundary; on the inlet and outlet the distribution functions f_i, g_i, t_i adopted the periodic boundary; and the inlet and the outlet pressure values are set to $P_{\text{in}} = 0.256$, $P_{\text{out}} = 0.0437$ through the function $h_i = E_i P$. At the section of Y $= 5$, the simulation results are shown in the contours of density, temperature, velocity, and pressure.

The six density contours at different moments of the center longitudinal section are shown in Fig. 1. In the legend, values 1 and 50 represent gas and liquid, respectively. When $t = 13{,}300$, phase change does not occur; the capillary tube is full of saturated liquid. When $t = 14{,}950$, the gas phase point appears at the center of the tube, where the phase change begins to occur. From the density contours at time steps of $t = 14{,}980$, $t = 15{,}140$, and $t = 15{,}240$, it is found that the gas increases continuously and expands along the center of the tube. The density contours shown in Fig. 2 indicate that the gas phase point appears firstly at the center of the tube, and it gathers into the gas mass. Then the gas mass develops increasingly along the tube; finally the center of the tube is almost full of gas.

As shown in Figs. 1(b)–1(d), both the front end and the back end of the gas masses have a round shape approximately, which can be seen as the result caused by limiting the development of the gas mass; it is similar to the phenomenon of restricted bubble flow found in a microchannel in the previous studies. With velocity and gas quantity increasing, a flow pattern similar to slug flow appears in Fig. 1(e). When further increases occur, gas masses flow

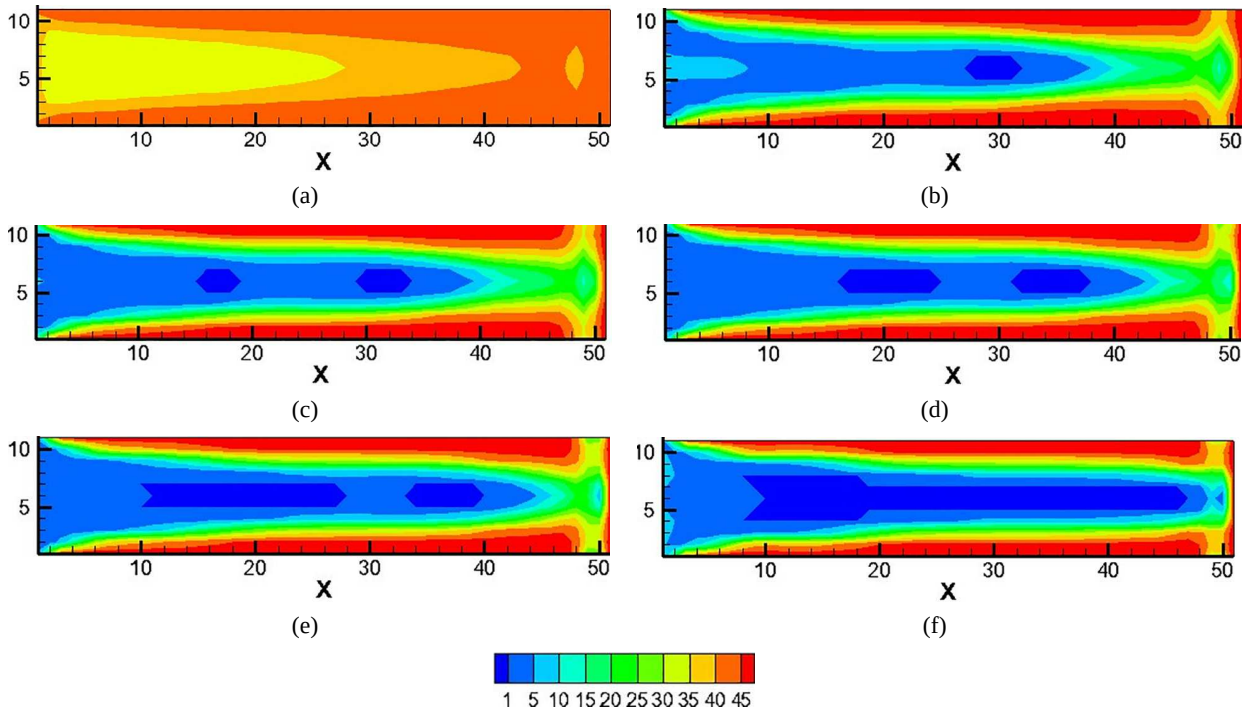

FIG. 1: Central longitudinal section density contours at different moments

along the center of the tube, while liquid flows close to the wall; the flow pattern of that belongs to annular flow. Yang et al. (2017) have done research on two-phase fluids in a 6-mm-diameter tube, where the medium is R600a, and slug flow and annular flow were found. The results are similar to those in this study.

3.2 Temperature Distribution

According to temperature distribution contours at different moments shown in Fig. 2, it is found that when t =13,300, the temperature of liquid at the center of the tube is higher than that of the wall. This indicates that there is a large superheating because of the high temperature at the center of the tube, where liquid nucleation happens easily. Therefore, areas of low density are formed firstly at the center of the tube, where phase change starts to occur. According to Figs. 1 and 2 when t = 14,950, the temperature of gas areas at the center of the tube decrease, which corresponds to the phenomenon that actually happens in capillary tubes. At the same time, according to Figs. 1 and 2 at t = 14,950 and t = 15,140 time steps, the temperature at the interface between gas and liquid is high, which indicates that because of the high temperature at the interface, refrigerant vapor can absorb heat from the interface continually in the process of phase change, until it evaporates completely into gas.

3.3 Velocity and Pressure Distribution

In Figs. 3 and 4, the velocity contour and pressure contour of the center longitudinal section are shown, when t = 15,240. The velocity contour shows that the velocity of fluid close to the wall is lower than that at the center. Because of the pressure gradient, the fluid velocity increases along the tube, and reaches a maximum value of 0.2

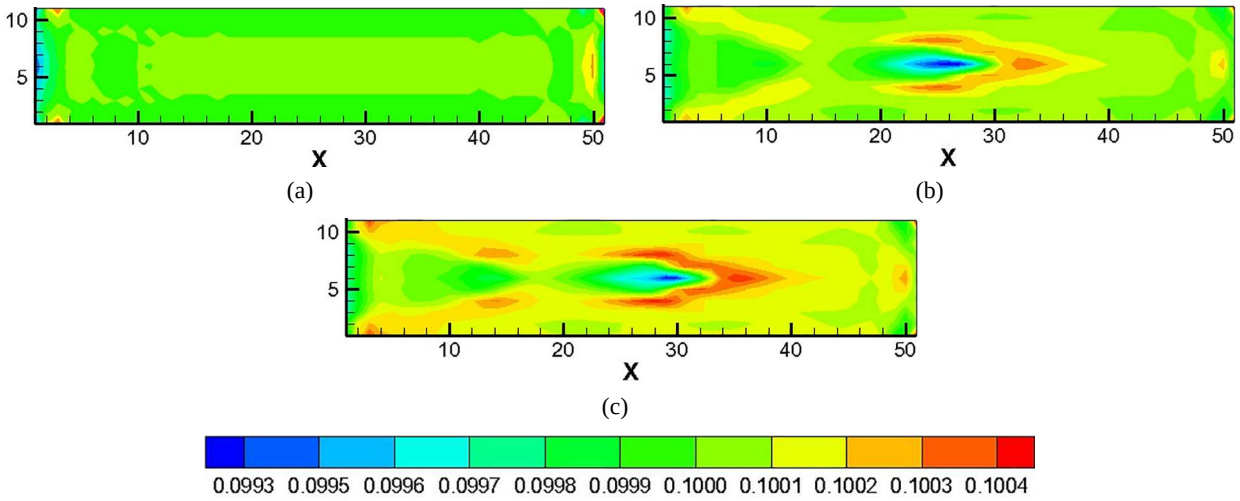

FIG. 2: Central longitudinal section temperature contours at different moments

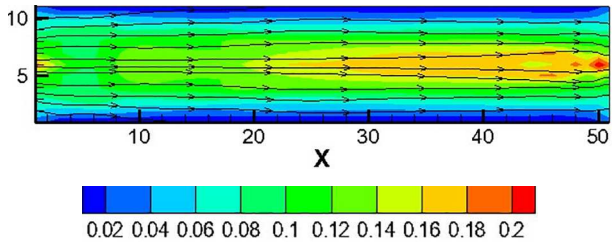

FIG. 3: Central longitudinal section velocity contour at t = 15,240

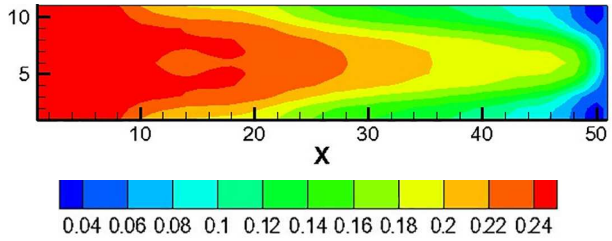

FIG. 4: Central longitudinal section pressure contour at $t = 15{,}240$

(corresponding actual physical quantity is 61 m/s) at the outlet. The value is close to 55 m/s, which is the result of numerical simulation of refrigerant flow along capillary tubes, as reported in the literature (Seixlack and Barbazelli, 2009). At the same time, the flow phenomenon corresponds to the rule of flow which has been driven by pressure in the capillary. According to Fig. 1(f), the density contour shows that there is a large gas area at the center of the tube. The velocity distribution of Fig. 3 shows that the velocity of gas in the central area is much higher than that of the liquid, which agrees with the phenomenon that the central region of the capillary is a high-speed zone (Zhou, 2003).

3.4 Influence of Pressure Drop

In order to analyze the effect of pressure drop on the flow in the tube, the flow field keeps the inlet pressure stable and changes the value of the outlet pressure. The values of outlet pressure are set as follows: 0.0437, 0.0599, 0.0898, 0.1197, 0.1496, and 0.1796, corresponding to the actual physical quantities of 0.73×10^5 Pa, 1×10^5 Pa, 1.5×10^5 Pa, 2×10^5 Pa, 2.5×10^5 Pa, and 3×10^5 Pa. Figure 5 shows the density distribution of the flow at the final state under

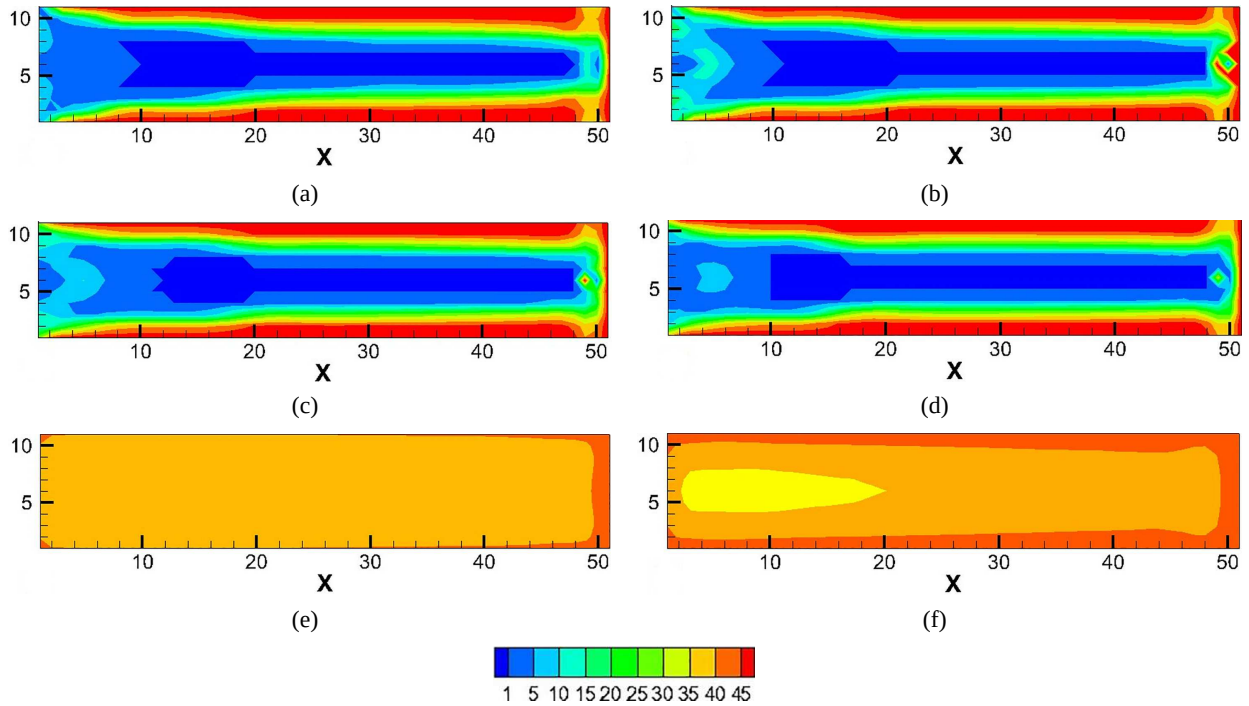

FIG. 5: The density distribution of the tube at the final state under different outlet pressures: (a) $P_{\text{out}} = 0.73 \times 10^5$ Pa; (b) $P_{\text{out}} = 1 \times 10^5$ Pa; (c) $P_{\text{out}} = 1.5 \times 10^5$ Pa; (d) $P_{\text{out}} = 2 \times 10^5$ Pa; (e) $P_{\text{out}} = 2.5 \times 10^5$ Pa; (f) $P_{\text{out}} = 3 \times 10^5$ Pa

different outlet pressure values. It is found in Figs. 5(a)–5(d) that, when $P_{out} = 0.73 \times 10^5$ Pa, $P_{out} = 1 \times 10^5$ Pa, $P_{out} = 1.5 \times 10^5$ Pa, and $P_{out} = 2 \times 10^5$ Pa, the density distribution contours of the flow are almost the same, and the center of the tube is almost full of gas at the final state. When the outlet pressure increases to 2.5×10^5 Pa and 3.0×10^5 Pa, the gas obviously decreases, and the tube is full of liquid, where phase change will not happen, as shown in Figs. 5(e) and 5(f). Therefore, within a certain range, the pressure drop of the flow along the tube has little effect on the liquid phase transition, but when it is beyond a certain range, the phase transition will be greatly reduced, or will not even occur.

4. CONCLUSIONS

Combining the free energy model with the thermal model, a hybrid LBM has been proposed and used to simulate two-phase fluids in a rectangular capillary tube. The following points are concluded from the present study:

1. From the results of the density distribution, the capillary tube throttling process is considered to start at the center of the tube, and then expands along the axial direction. Finally, the center of the tube is almost filled with the gas. In the process of flow, the flow patterns similar to slug flow pattern and annular flow pattern appear.

2. The temperature at the interface between gas and liquid is high, which indicates that because of the high temperature at the interface, refrigerant vapor can absorb heat from the interface continually in the process of phase change, until it evaporates completely into gas.

3. The fluid velocity increases along the tube, and reaches a maximum value of 61 m/s. The velocity of gas is much higher than that of liquid in the capillary tube.

4. Within a certain range, the pressure drop of the flow along the tube has little effect on the liquid phase transition, but when it is beyond a certain range, the phase transition will be greatly reduced, or will not even occur.

ACKNOWLEDGMENTS

This work was financially supported by National Natural Science Foundation of China (No. 50976015), Liaoning S&T project (No. 2010224002), and the Fundamental Research Funds for the Central Universities (3132016338).

REFERENCES

Bolstad, M.M. and Jordan, R.C., Theory and Use of the Capillary Tube Expansion Device, *J. Refrig. Eng*., vol. **56**, no. 12, pp. 577–583, 1948.

Cooper, L., Chu, C.K., and Bresken, W.R., Simple Selection Method for Capillaries Derived from Physical Flow Condition, *J. Refrig. Eng*., vol. **65**, pp. 37–41, 1957.

Deodhar, S.D., Kothadia, H.B., Iyer, K.N., and Prabhu, S.V., Experimental and Numerical Studies of Choked Flow through Adiabatic and Diabatic Capillary Tubes, *J. Appl. Therm. Eng*., vol. **90**, pp. 879–894, 2015.

Ewing, M.E., Weinandy, J.J., and Christensen, R.N., Observations of Two-Phase Flow Patterns in a Horizontal Circular Channel, *J. Heat Transf. Eng.*, vol. **20**, no. 1, pp. 9–14, 1999.

Fiorelli, F.A.S., Huerta, A.A.S., and Silvares, O.D.M., Experimental Analysis of Refrigerant Mixtures Flow through Adiabatic Capillary Tubes, *J. Exp. Therm. Fluid Sci*., vol. **26**, no. 5, pp. 499–512, 2002.

Huang, J., Xiao, F., and Yin, X., Lattice Boltzmann Simulation of Pressure-Driven Two-Phase Flows in Capillary Tube and Porous Medium, *J. Comput. Fluids*, vol. **155**, pp. 134–145, 2017.

Inamuro, T., Ogata, T., Tajima, S., and Konishi, N., A Lattice Boltzmann Method for Incompressible Two-Phase Flows with Large Density Differences, *J. Comput. Phys*., vol. **198**, no. 2, pp. 628–644, 2004.

Inamuro, T., Lattice Boltzmann Methods for Viscous Fluid Flows and Two-Phase Fluid Flows, *J. Fluid Dyn. Res*., vol. **38**, no. 9, pp. 654–659, 2006.

Khan, M.K., Kumar, R., and Sahoo, P.K., Flow Characteristics of Refrigerants Flowing through Capillary Tubes—A Review, *J. Appl. Therm. Eng*., vol. **29**, nos. 8-9, pp. 1426–1439, 2009.

Koizumi, H. and Yokoyama, K., Characteristics of Refrigerant Flow in a Capillary Tube, *ASHRAE Trans*., vol. **86**, no. 2, pp. 19–27, 1980.

Liu, Q., Wang, W., and Palm, B., A Numerical Study of the Transition from Slug to Annular Flow in Micro-Channel Convective Boiling, *J. Appl. Therm. Eng*., vol. **112**, pp. 73–81, 2016.

Oliveira, J.D.D., Copetti, J.B., and Passos, J.C., An Experimental Investigation on Flow Boiling Heat Transfer of R-600a in a Horizontal Small Tube, *J. Int. J. Refrig*., vol. **72**, pp. 97–110, 2016.

Revellin, R., Dupont, V., Ursenbacher, T., Thome, J.R., and Zun, I., Characterization of Diabatic Two-Phase Flows in Microchannels: Flow Parameter Results for R-134a in a 0.5 mm Channel, *J. Int. J. Multiphase Flow*, vol. **32**, no. 7, pp. 755–774, 2006.

Schenk, M. and Oellrich, L.R., Experimental Investigation of the Refrigerant Flow of Isobutene (R600a) through Adiabatic Capillary Tubes, *J. Int. J. Refrig*., vol. **38**, no.1, pp. 275–280, 2014.

Seixlack, A.L. and Barbazelli, M.R., Numerical Analysis of Refrigerant Flow Along Non-Adiabatic Capillary Tubes using a Two-Fluid Model, *J. Appl. Therm. Eng*., vol. **29**, nos. 2-3, pp. 523–531, 2009.

Staebler, L.A., Theory and Use of a Capillary Tube for Liquid Refrigerant Control, *J. Refrig. Eng*., vol. **55**, pp. 55–59, 1948.

Triplett, K.A., Ghiaasiaan, S.M., Abdel-Khalik, S.I., and Sadowski, D.L., Gas–Liquid Two-Phase Flow in Microchannels Part I: Two-Phase Flow Patterns, *Int. J. Multiphase Flow*, vol. **25**, no. 3, pp. 377–394, 1999.

Wongwises, S., Songnetichaovalit, T., Lokathada, N., Kritsadathikarn, P., Suchatawat, M., and Pirompak, W., A Comparison of the Flow Characteristics of Refrigerants Flowing through Adiabatic Capillary Tubes, *J. Int. Commun. Heat Mass Transf.*, vol. **27**, no. 5, pp. 611–621, 2000.

Yang, Z., Gong, M., Chen, G., Zou, X., and Shen, J., Two-Phase Flow Patterns, Heat Transfer and Pressure Drop Characteristics of R600a during Flow Boiling inside a Horizontal Tube, *J. Appl. Therm. Eng*., vol. **120**, pp. 654–671, 2017.

Zhou, Q., Study on the Flow Characteristics of Refrigerants in Capillary Tubes, MS thesis, Zhejiang University, 2003.